# Downregulation of *OCLN* and *GAS1* in clear cell renal cell carcinoma

ANDRÉ LUIS GIACOMETTI CONCEIÇÃO[1], CAMILA TAINAH DA SILVA[2], RODOLFO MIGLIOLI BADIAL[1], MARINA CURADO VALSECHI[1], BRUNA STUQUI[1], JÉSSICA DOMINGUES GONÇALVES[2], MIRIAM GALVONAS JASIULIONIS[2], MARILIA DE FREITAS CALMON[1] and PAULA RAHAL[1]

[1]Laboratory of Genomic Studies, Department of Biology, São Paulo State University (UNESP), São José do Rio Preto, SP 15054-000; [2]Department of Pharmacology, The Federal University of São Paulo (UNIFESP), São Paulo, SP 15054-000, Brazil

Received September 21, 2016; Accepted November 3, 2016

DOI: 10.3892/or.2017.5414

**Abstract.** Clear cell renal cell carcinoma (ccRCC) is the most common histological subtype of kidney cancer. This carcinoma is histologically characterized by the presence of clear and abundant cytoplasm. In the present study, we sought to identify genes differentially expressed in ccRCC and build a molecular profile of this cancer. We selected genes described in the literature related to cellular differentiation and proliferation. We analyzed the gene and protein expression by quantitative PCR (qPCR) and immunohistochemistry, respectively, and examined possible epigenetic mechanisms that regulate their expression in ccRCC samples and cell lines. Occludin (*OCLN*) and growth arrest-specific 1 (*GAS1*) genes were underexpressed in ccRCC, and we report that miR-122 and miR-34a, respectively, may regulate their expression in this cancer. Furthermore, we showed by qPCR and immunohistochemistry that solute carrier family 2 member 1 (*SLC2A1*) was significantly overexpressed in ccRCC. The set of genes identified in the present study furthers our understanding of the molecular basis and development of ccRCC.

## Introduction

Clear cell renal cell carcinoma (ccRCC) is the most common histological subtype of kidney cancer in adults (70-75% of cases) (1). Approximately 30% of early-stage patients develop metastases after surgery for localized disease (2). This carcinoma is histologically characterized by the presence of clear and abundant cytoplasm (2,3). The aggressive characteristics of renal clear cell carcinoma interfere in the efficiency of conventional treatment approaches, such as chemotherapy and radiotherapy (4).

Mutations or deletions associated with tumor suppressor genes may cause the loss or inactivation of these negative regulators. However, the loss of function may be caused by epigenetic changes (5), including acetylation, methylation, phosphorylation, ubiquitinylation, sumoylation, carbonylation and regulation of microRNAs (6). Epigenetic alterations occur at a high frequency, are reversible upon treatment with pharmacological agents and arise at defined regions within a gene (7,8). These features make epigenetics a very attractive field for cancer detection and several studies have shown multiple genes with different types of epigenetic alterations in tumor tissue (9-11).

Analyzing the gene expression and regulatory mechanisms in tumor samples has shown great efficiency in providing new information on signaling pathway activation of several processes, such as evasion of apoptosis, angiogenesis and metastatic potential.

The occludin (*OCLN*) gene, responsible for producing the protein occludin, is known to be present in all the tight junctions (TJs). TJ formation and expression has been described as a hallmark of epithelial cells and their subsequent loss from cancer cells tends to be considered as a direct effect of epithelial-mesenchymal transition (EMT) (12). Furthermore, occludin is structurally connected to the TGF-β receptor contributing to essential changes in EMT cell phenotype (13).

Growth arrest-specific 1 (*GAS1*) gene is associated with cell arrest and the protein is linked to the outer cell membrane by a glycosyl phosphatydylinositol. GAS1 protein binds to Hedgehog ligands for the potentiation of Hedgehog signaling (14).

Solute carrier family 2 member 1 (*SLC2A1*) gene encodes the solute carrier family 2 facilitated glucose transporter member 1 protein essential for cellular energy metabolism pathways (15-17). This protein is able to develop bidirectional flow of glucose according to the gradient of the substrate. The overexpression of the SLC2A1 protein has been found to be involved in increased uptake of glucose in human breast adenocarcinoma cell lines (18).

*Correspondence to:* Professor Paula Rahal, Laboratory of Genomic Studies, Department of Biology, São Paulo State University (UNESP), 2265 Cristóvão Colombo, São José do Rio Preto, SP 15054-000, Brazil
E-mail: rahalp@yahoo.com.br

*Key words:* clear cell renal cell carcinoma, gene expression, miRNA, epigenetic, ChIP, immunohistochemistry

In the present study, we selected genes described in the literature related to cellular differentiation and proliferation. We analyzed their expression by quantitative PCR (qPCR) and immunohistochemistry, and examined the possible epigenetic mechanisms that regulate genes in ccRCC samples and cell lines. *OCLN* and *GAS1* were underexpressed in ccRCC and miR-122 and miR-34a may regulate their expression in this type of cancer. Furthermore, we showed by qPCR and immunohistochemistry that *SLC2A1* was significantly overexpressed in ccRCC samples. These genes may be involved in the molecular biology and development of the disease and analysis of them may contribute to insights for new prognoses, treatments and understanding this type of tumor.

## Materials and methods

*ccRCC samples*. The samples were collected from 101 patients diagnosed with ccRCC, including 45 fresh samples of ccRCC, 56 paraffin-embedded samples of ccRCC, 2 fresh-frozen histologically healthy renal tissue and 24 paraffin-embedded samples of histologically healthy renal tissues, all of which were confirmed by pathologists (Tables I and II). The samples were obtained from the Hospital de Base at Faculdade de Medicina de São José do Rio Preto (Sao Paulo, Brazil). The use of patient-derived material was approved by the Research Ethics Committee of the IBILCE-UNESP and FAMERP (Sao Paulo, Brazil) and written consent was obtained from all the patients. Tissues were obtained from patients undergoing tumor resection surgery, and a diagnosis of ccRCC was determined post-operatively using histopathology. The samples were classified according to the criteria provided by the International Union against Cancer (19).

*Cell lines and treatments*. The 786-O (primary clear cell adenocarcinoma) cell line was obtained from the American Type Culture Collection (ATCC; Manassas, VA, USA) and HaCaT (an immortal human keratinocyte cell line) was kindly provided by Luisa Lina Villa (Department of Radiology, Center of Translational Oncology Investigation, São Paulo State Cancer Institute, Universidade de São Paulo, Brazil). 786-O cells were cultured in RPMI-1640 medium, and HaCaT cells were cultured in Dulbecco's modified Eagle's medium (DMEM) (both from Gibco by Life Technologies, Grand Island, NY, USA). The media were supplemented with 10% fetal bovine serum (Cultilab, Sao Paulo, Brazil), 100 U/ml of penicillin and 100 $\mu$g/ml of streptomycin (both from Invitrogen, Grand Island, NY, USA). Cell cultures were grown at 37˚C in a 5% $CO_2$ atmosphere. 786-O cells were plated into 6-well plates, cultured for 24 h, and treated for 72 h with fresh 5, 2 or 1 $\mu$M of 5-Aza-dC (Sigma-Aldrich, St. Louis, MO, USA) dissolved in phosphate-buffered saline. Due to its chemical instability, fresh medium with 5-Aza-dC was added every 24 h. For the trichostatin A (TSA) experiments, the cells were seeded in 6-well plates, cultured for 24 h, and treated for 24 h with fresh 1,000, 500, 300, 200 or 100 nM of TSA (Sigma-Aldrich) dissolved in dimethyl sulfoxide (DMSO). To assess the combined effect of both drugs, we performed the co-treatment of cells with 5 $\mu$M of 5-Aza-dC and 1,000 nM of TSA using the following protocol: 5-Aza-dC was added for 72 h, after which it was removed and

Table I. Epidemiological and clinicopathological characteristics of the patients diagnosed with ccRCC (fresh samples).

| Sample | Gender | Age (years) | Alcohol | Smoking | TNM |
|---|---|---|---|---|---|
| F1 | M | 58 | No | No | T1N1M1 |
| F2 | F | 39 | No | No | T2N0M0 |
| F3 | F | 71 | No | No | T4N0M1 |
| F4 | F | 64 | No | No | T2N0M0 |
| F5 | M | 46 | No | No | T1bN0M0 |
| F6 | M | 70 | No | No | T2N0M0 |
| F7 | M | 70 | Yes | Yes | T3aN0M0 |
| F8 | F | 58 | Yes | Yes | T3N3M1 |
| F9 | M | 36 | No | No | T1aN0M0 |
| F10 | M | 48 | Yes | No | T2N0M0 |
| F11 | M | 52 | No | No | T3aN0M0 |
| F12 | F | 62 | No | No | T1aN0M0 |
| F13 | M | 75 | No | Yes | T1N0M0 |
| F14 | F | 49 | No | No | T1bN0M0 |
| F15 | F | 71 | No | No | T1N0M0 |
| F16 | F | 79 | No | No | T1aN0M0 |
| F17 | F | 29 | No | No | T2N0M0 |
| F18 | M | 70 | No | No | T2N0M0 |
| F19 | M | 39 | No | Yes | T2N0M0 |
| F20 | M | 66 | Yes | No | T2N0M0 |
| F21 | M | 77 | No | No | T2N0M1 |
| F22 | F | 23 | No | No | T2N0M0 |
| F23 | F | 53 | No | No | T2N0M0 |
| F24 | M | 69 | No | No | T3N0M0 |
| F25 | F | 60 | No | No | T3bN0M1 |
| F26 | F | 79 | No | No | T3aN0M0 |
| F27 | F | 59 | No | No | T2N0M0 |
| F28 | F | 64 | No | No | T1N0M0 |
| F29 | M | 53 | Yes | No | T2N0M0 |
| F30 | M | 56 | Yes | No | T1N1M1 |
| F31 | M | 54 | No | No | T2N0M0 |
| F32 | M | 52 | Yes | No | T1aN0M0 |
| F33 | M | 67 | Yes | No | T1aN0M0 |
| F34 | M | 41 | No | Yes | T1N0M0 |
| F35 | F | 55 | No | No | T3aN2M1 |
| F36 | F | 52 | Yes | Yes | T3aNxMx |
| F37 | F | 25 | No | Yes | NI |
| F38 | M | 56 | No | No | T1bN0Mx |
| F39 | F | 83 | No | No | T1N0M0 |
| F40 | M | 68 | Yes | Yes | NI |
| F41 | F | 71 | No | Yes | T1bNxMx |
| F42 | M | 73 | No | Yes | T3NxM1 |
| F43 | M | 63 | Yes | No | T3aN0M0 |
| F44 | M | 62 | Yes | Yes | NI |
| F45 | M | 39 | Yes | No | T2NxM0 |

M, male; F, female; NI, no information was obtained. ccRCC, clear cell renal cell carcinoma; TNM, tumor-node-metastasis.

Table II. Epidemiological and clinicopathological characteristics of the patients diagnosed with ccRCC (paraffin-embedded samples).

| Sample | Gender | Age (years) | Alcohol | Smoking | TNM |
|---|---|---|---|---|---|
| P1 | M | 80 | No | No | T4N1M1 |
| P2 | M | 50 | No | No | T2N0M0 |
| P3 | M | 61 | No | No | T3bN0M0 |
| P4 | F | 69 | No | No | T1bN0M0 |
| P5 | M | 52 | No | Yes | T2N0M0 |
| P6 | M | 88 | No | Yes | T2N0M0 |
| P7 | M | 60 | No | No | T1bN0M0 |
| P8 | M | 58 | No | No | T1bN1M1 |
| P9 | M | 71 | No | Yes | T1N0M0 |
| P10 | M | 56 | No | No | T3bN0M1 |
| P11 | M | 77 | No | No | T2N1M1 |
| P12 | F | 32 | Yes | No | T1aN0M0 |
| P13 | M | 68 | No | No | T3bN0M0 |
| P14 | M | 83 | Yes | Yes | T2N0M1 |
| P15 | F | 65 | No | No | T2N0M0 |
| P16 | F | 54 | No | No | T1bN0M0 |
| P17 | M | 44 | NI | NI | NI |
| P18 | M | 65 | No | No | T3aN0M1 |
| P19 | F | 72 | No | Yes | T2N0M1 |
| P20 | F | 60 | No | No | T2N0M0 |
| P21 | M | 77 | No | No | T1bN0M0 |
| P22 | M | 52 | No | No | T1bN0M0 |
| P23 | M | 74 | No | No | T3aN0M1 |
| P24 | M | 75 | No | No | T2N0M0 |
| P25 | M | 78 | No | No | T2N0M0 |
| P26 | F | 66 | No | No | T2N0M0 |
| P27 | M | 64 | No | No | T1bN0M0 |
| P28 | M | 67 | Yes | Yes | T2N0M0 |
| P29 | M | 49 | No | No | T2N0M0 |
| P30 | F | 58 | No | No | T1bN0M0 |
| P31 | M | 84 | No | Yes | T1bN0M0 |
| P32 | F | 48 | No | Yes | T2N0M0 |
| P33 | F | 55 | No | No | T1bN0M0 |
| P34 | F | 50 | No | No | T2N0M0 |
| P35 | F | 46 | No | No | T1aN0M0 |
| P36 | M | 43 | No | No | T2N0M0 |
| P37 | F | 54 | No | Yes | T3aN0M0 |
| P38 | F | 86 | No | Yes | T3N0M0 |
| P39 | M | 51 | No | No | T2N0M0 |
| P40 | M | 74 | No | No | T2N0M0 |
| P41 | F | 51 | No | Yes | T1aN0M0 |
| P42 | M | 63 | Yes | Yes | T3aN0M0 |
| P43 | M | 56 | No | No | T2N0M0 |
| P44 | F | 76 | No | Yes | T1bNxMx |
| P45 | M | 70 | No | Yes | T1aNxMx |
| P46 | M | 58 | No | No | T1bN0M0 |
| P47 | M | 56 | No | No | T1bN0M0 |
| P48 | M | 76 | No | No | T3N0M0 |
| P49 | F | 61 | No | No | NI |
| P50 | M | 81 | Yes | No | NI |
| P51 | M | 76 | Yes | Yes | T2N0M0 |
| P52 | F | 72 | No | No | T1N0M0 |
| P53 | F | 79 | No | No | T2N0M0 |
| P54 | M | 59 | No | Yes | T2N0M0 |
| P55 | M | 46 | No | No | T2N0M1 |
| P56 | F | 89 | No | Yes | T1N0M0 |

M, male; F, female; NI, no information was obtained. ccRCC, clear cell renal cell carcinoma; TNM, tumor-node-metastasis.

TSA was added for an additional 24 h. All experiments were performed in triplicate.

*Cytotoxicity assay*. 786-O cells were seeded into 96-well plates at a density of $10^3$ cells for 5-Aza-dC treatment, $10^4$ cells for TSA and $5x10^3$ cells for co-treatment. After the 5-Aza-dC and TSA treatments, 1 mg/ml of 3-(4,5-dimethylthiazol-2-yl)-2,5-diphenyltetrazolium bromide (MTT) (Sigma-Aldrich) was added to each well and incubated for 30 min at 37˚C. Then, the MTT was removed and 100 $\mu$l of 100% DMSO (Sigma-Aldrich) was added to each well and the absorbance was measured at 562 nm. Each experiment was performed in triplicate and in 2 independent assays.

*RNA and DNA extraction*. Genomic DNA and total RNA extraction were performed using TRIzol® reagent (Life Technologies) using both cell lines, the 45 fresh samples of ccRCC and 2 fresh-frozen histologically healthy renal tissue samples, following the manufacturer's instructions. The DNA and RNA quality was verified by electrophoresis through an agarose gel and stained with ethidium bromide. For quantitative real-time PCR, 5 $\mu$g of total RNA from each sample was used to synthesize cDNA with a High-Capacity cDNA Archive kit (Applied Biosystems, Foster City, CA, USA), according to the manufacturer's instructions. The cDNA quality was ascertained by PCR using the housekeeping gene *β-actin*. The PCR products were analyzed by electrophoresis on a 1% agarose gel and stained with ethidium bromide.

*Selection of genes*. We analyzed the differential expression of the following genes by qPCR: E-cadherin (*CDH1*), N-cadherin (*CDH2*), claudin 1 (*CLDN1*), cathepsin B (*CTSB*), platelet-activating factor acetylhydrolase 2 (*PAFAH2*), growth arrest-specific 1 (*GAS1*), laminin β1 (*LAMβ1*), occludin (*OCLN*), phosphoglycerate dehydrogenase (*PHGDH*), solute carrier family 2 member 1 (*SLC2A1*), transforming growth factor β1 (*TGFβ1*), tight junction protein 1 (*TJP1*) and vimentin (*VIM*). The genes were selected according to their role in cellular differentiation and proliferation.

*Quantitative real-time polymerase chain reaction*. The qPCR amplification was performed with Power SYBR-Green and an ABI 7300 Real-Time PCR System (Applied Biosystems, Warrington, UK). In brief, the reaction mixture (20 $\mu$l of total volume) contained 25 ng of cDNA, gene-specific forward and reverse primers and 10 $\mu$l of 2X Quantitative SYBR-Green PCR Master Mix. The samples were tested in triplicate. The relative expression of each specific gene was calculated using the following previously published (20) formula: $R = (E\ target)^{\Delta Ct\ target\ (control\ -\ sample)}/(E\ endogenous^{\Delta Ct\ endogenous\ (control\ -\ sample)}$. A 2-fold-change was set as the cut-off. Gene expression was analyzed in 45 ccRCC samples, in the 786-O cells after treatment and the HaCaT cell line. Two healthy renal fresh-frozen tissue samples were used as the healthy reference (control group). A non-treated 786-O cell line was used as a reference sample and *GAPDH* was selected as the endogenous control gene.

*Bisulfite sequencing*. Genomic DNA was subjected to a sodium bisulfite treatment to modify unmethylated cytosine to uracil, as described by Calmon *et al* (21). Bisulfite-treated DNA was amplified by PCR, using primers designed to amplify CpG-rich regions located at the 5' region of *OCLN* (-438 to +1232, relative to the transcription start site (TSS) and encompassing 164 CpG dinucleotides] and *GAS1* [-485 to +1518, relative to the TSS and encompassing 269 CpG dinucleotides). The amplified products were cloned using a CloneJET PCR Cloning kit (Thermo Scientific, Carlsbad, CA, USA). Five positive clones from the 786-O cell line before and after treatment with 5-Aza-dC, one ccRCC sample and one healthy renal sample were sequenced using a BigDye Terminator v3.1 Cycle Sequencing kit and an ABI3130XL sequencer, according to the manufacturer's instructions (Applied Biosystems). The methylation percentage for each sample was calculated as the proportion of unconverted CpG dinucleotides among all of the CpG dinucleotides analyzed from the 5 positive clones.

*Chromatin immunoprecipitation (ChIP)*. ChIP was performed using a ChIP-IT® High Sensitivity kit according to the manufacturer's instructions (Active Motif, Carlsbad, CA, USA). The 786-O and HaCaT cells were cross-linked with 1% formaldehyde for 10 min at room temperature and nuclei were isolated. Isolated nuclei were sonicated on ice to break the chromatin into 8,200-1,200 bp fragments. Soluble chromatin was used in immunoprecipitation with H3K4me3, H3K27me3, H3K4me2 and H3K9ac antibodies (Thermo Scientific, Rockford, IL, USA). IgG was used as a negative control (Abcam, Cambridge, MA, USA) and immune complexes were absorbed with protein G magnetic beads. After reversing the cross-linking and treating with proteinase K, the immunoprecipitated DNA was analyzed on a gene-specific basis using qPCR. The quality control ChIP was performed using a ChIP-IT® qPCR Analysis kit (Active Motif) with Human Negative Control Primer Set 1 and Human Positive Control Primer Set GAPDH-2, according to the manufacturer's instructions.

*MicroRNA analysis*. Two microRNA databases, miRBase (www.mirbase.org) and TargetScanHuman (www.targetscan.org), were used to select microRNAs that target the *OCLN* and *GAS1* mRNA. For microRNA expression analysis, total RNA was reverse transcribed into cDNA using miR-34a, miR-122 and U48-specific steam-loop primers. Expression of mature miR-34a and miR-122 was quantified as described in the qPCR methods. The microRNA expression was analyzed in 30 ccRCC samples and in the cell lines 786-O and HaCaT. Two healthy renal fresh-frozen tissue samples were used as a healthy reference. Each sample was run in triplicate, and the miRNA expression levels were normalized to U48.

*Tissue array construction and immunohistochemistry*. Tissue microarrays were constructed using a tissue microarrayer (Beecher Instruments, Silver Spring, MD, USA). Briefly, the slides were reviewed by a pathologist, and areas containing each category were annotated on the hematoxylin and eosin (H&E) slides. Fifty-six 1.0 mm in diameter cylindrical tissue cores from the ccRCC tumor samples and 24 from the tumor margins were taken from the corresponding regions of the paraffin blocks and transplanted into a recipient paraffin block.

For immunohistochemical staining, all of the paraffin-embedded sections were cut into 4-$\mu$m in thickness and the endogenous peroxidase activity was blocked with 3% hydrogen peroxide for 30 min. Antigen retrieval was performed using sodium citrate buffer (pH 6,0) for 20 min at 96˚C in a steam pan. The sections were then incubated with SLC2A1 polyclonal primary antibody (1:200) (Abcam) diluted in 1% BSA at 4˚C overnight. After incubation with a primary antibody, the sections were incubated with a biotinylated secondary antibody (Santa Cruz Biotechnology, Paso Robles, CA, USA) and then exposed to a streptavidin complex (HRP ready-to-use; DakoCytomation, Carpinteria, CA, USA). Positive staining was identified using DAB substrate color detection (Dako, Cambridge, UK). The sections were counterstained with hematoxylin.

The SLC2A1 densitometric analyses were conducted with an Axioskop II microscope using the Axiovision™ software (both from Zeiss, Oberkochen, Germany) . For these analyses, 20 different points were analyzed from 3 different fields of each tumor fragment and the average immunoreactivity intensity [arbitrary units (AU)] was recorded.

*Statistical analysis*. Statistical analyses were performed using GraphPad Prism 5 Software (GraphPad Software Inc., San Diego, CA, USA). The relative expression levels detected by qPCR in ccRCC were transformed into natural logarithms. The Wilcoxon signed-rank test was applied to compare the gene expression levels in tumor and healthy tissues. The Mann-Whitney U test and Wilcoxon signed-ranks tests were used to compare the protein expression levels detected by immunohistochemistry.

## Results

*Evaluation of EMT gene expression in ccRCC*. To evaluate gene expression in 45 ccRCC fresh samples and the 786-O cell line, we performed qPCR for the following target genes: *CDH1*, *CDH2*, *CLDN1*, *CTSB*, *PAFAH2*, *GAS1*, *LAMβ1*, *OCLN*, *PHGDH*, *SLC2A1*, *TGFβ1*, *TJP1* and *VIM*.

*CDH2*, *CTSB*, *GAS1*, *LAMβ1*, *OCLN*, *PHGDH*, *PAFAH2* and *TJP1* were significantly downregulated in the ccRCC samples when compared to the reference samples. *SLC2A1* was

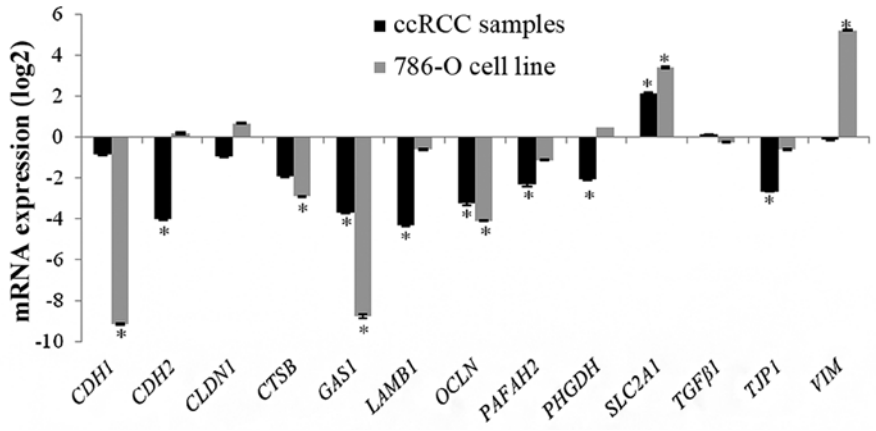


Figure 1. Gene expression profile in ccRCC tissues. mRNA expression of the selected genes using qPCR in 45 ccRCC fresh samples and in the 786-O cell line. The results are shown as the fold-change in the expression relative to the healthy sample (*p<0.001; Wilcoxon signed-rank test).

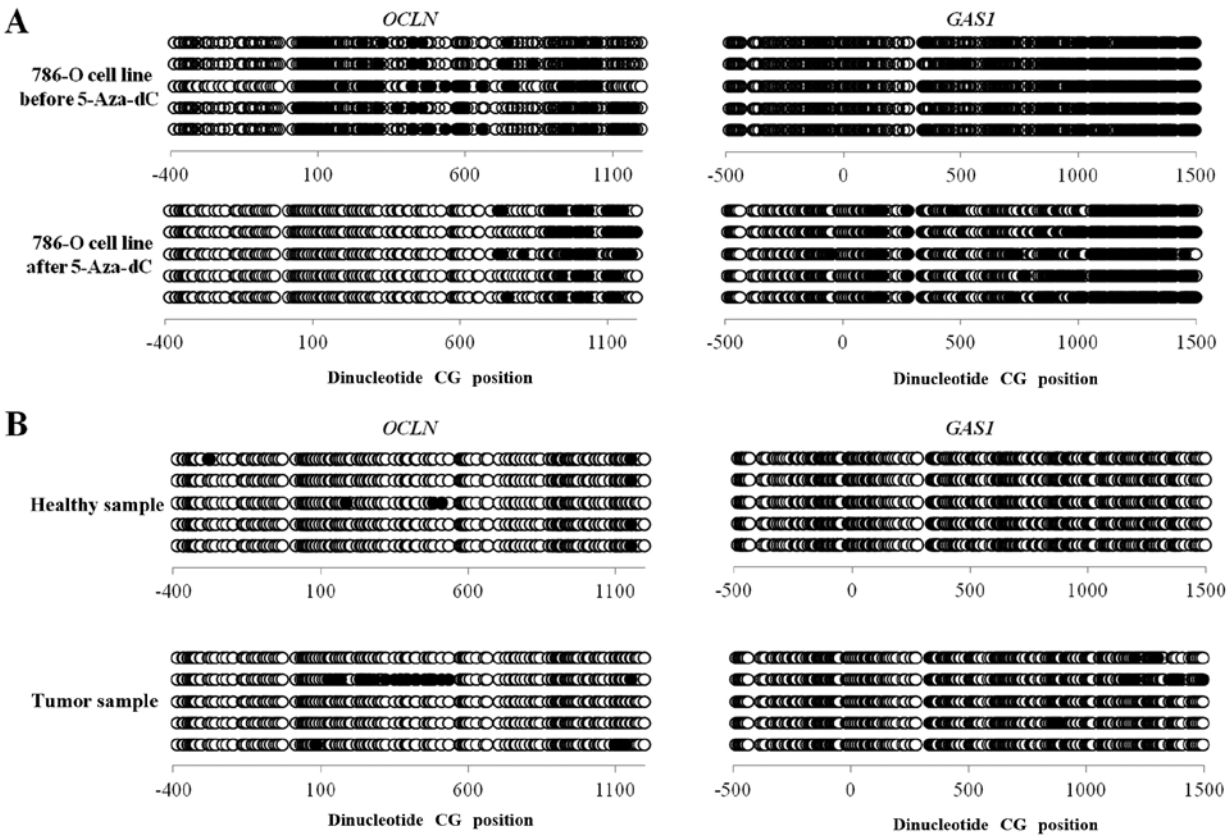


Figure 2. Methylation levels in *OCLN* and *GAS1* gene promoters. The transcription initiation site is represented by +1. An expanded view shows the position of CpG islands and the region analyzed by bisulfite sequencing. Each row represents one sequenced clone, and open circles and filled circles represent unmethylated and methylated CpG dinucleotides, respectively. (A) Bisulfite sequencing of *OCLN* and *GAS1* before and after 5-Aza-dC treatment. (B) Bisulfite sequencing of *OCLN* and *GAS1* in healthy and tumor samples.

significantly overexpressed in tumor tissues when compared to healthy renal tissues. *CDH1*, *TGFβ1*, *VIM* and *CLDN1* were not differentially expressed (Fig. 1).

*CDH1*, *CTSB*, *GAS1* and *OCLN* were significantly downregulated in 786-O cells. *SLC2A1* and *VIM* were significantly overexpressed in 786-O cells. *CDH2*, *CLDN1*, *LAMβ1*, *PAFAH2*, *PHGDH*, *TGFβ1* and *TJP1* were not differentially expressed (Fig. 1).

*OCLN* and *GAS1* were chosen for epigenetic analysis due to the presence of CpG islands in their promoter regions and the observed downregulation in both the ccRCC samples and 786-O cells. *SLC2A1* was selected for immunohistochemical analysis since it was overexpressed in both the ccRCC samples and 786-O cells.

*DNA methylation and histone acetylation analysis*. The methylation status of CpG islands at the 5' region of the *OCLN* and *GAS1* genes was investigated by bisulfite sequencing in ccRCC samples, healthy renal tissue and 786-O cells before and after 5-Aza-dC treatment. The bisulfite sequencing was performed

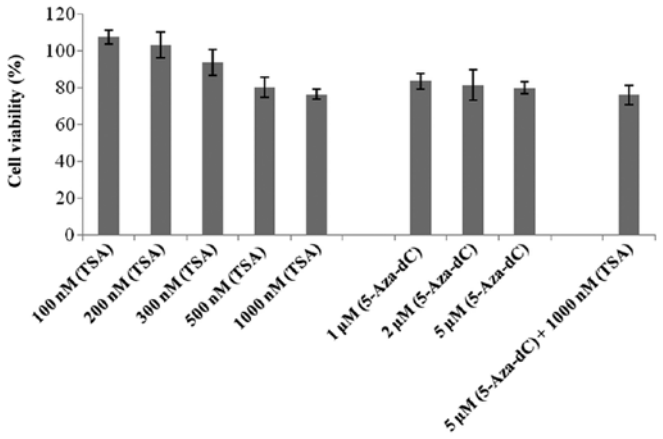


Figure 3. 786-O cell viability after 5-Aza-dC and TSA treatment. Cell viability of 786-O cells after 5-Aza-dC, TSA and co-treatment with 5-Aza-dC and TSA.

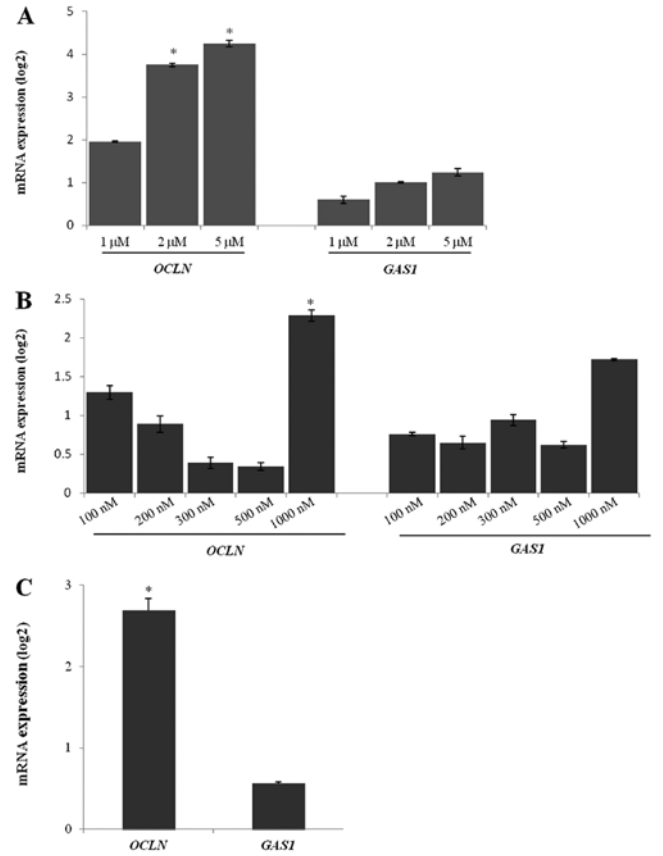


Figure 4. *OCLN* and *GAS1* expression levels after 5-Aza-dC and TSA treatment. (A) mRNA expression of *OCLN* and *GAS1* genes in the 786-O cell line after 5-Aza-dC treatment. (B) mRNA expression of *OCLN* and *GAS1* genes in the 786-O cell line after TSA treatment, (C) mRNA expression of *OCLN* and *GAS1* in the 786-O cell line after co-treatment with 5-Aza-dC and TSA (*p<0.001; Wilcoxon signed-rank test).

in the -438 to +1232 region of *OCLN* and the -485 to +1518 region of *GAS1*. The methylation levels of *OCLN* and *GAS1* were not significantly reduced in 786-O cells before and after 5 $\mu$M of 5-Aza-dC treatment (24.39-22.19% for *OCLN* and 22.5-22.23% for *GAS1*). The methylation level of the genes compared between the ccRCC samples and the healthy renal samples did not significantly differ, 4-1% for *OCLN* and 1.8-0% for *GAS1* (Fig. 2).

An MTT assay was performed to detect the possible effects of 5-Aza-dC and TSA treatment on 786-O cell viability. All of the drug concentrations tested showed viability >75%, including the co-treatment (Fig. 3).

The cell growth was inhibited in a dose-dependent manner by 5-Aza-dC treatment in 786-O cells. The expression of *OCLN* mRNA was higher in the cells treated with 5 and 2 $\mu$M of 5-Aza-dC than in the untreated cells (Fig. 4A). There was no difference in the *GAS1* mRNA expression after treatment with any 5-Aza-dC concentration (Fig. 4A).

Similar to the 5-Aza-dC treatment, TSA treatment showed a better response at the highest concentration (1,000 nM). The *OCLN* gene was upregulated in the 786-O cells after 1,000 nM TSA treatment when compared to the untreated cells (Fig. 4B). Other TSA concentrations were not able to significantly upregulate *OCLN* expression. The *GAS1* expression levels were unchanged after TSA treatment in 786-O cells when compared to the untreated cells (Fig. 4B).

The 5-Aza-dC (5 $\mu$M) and TSA (1,000 nM) co-treatment efficiently upregulated *OCLN* expression in 786-O cells. However, *GAS1* gene expression was not altered after co-treatment (Fig. 4C).

*ChIP*. Since there was alteration in the *OCLN* gene expression after 5-Aza-dC treatment without any difference in the DNA methylation level in its promoter region and it is known that 5-Aza-dC treatment may alter both DNA and histone methylation (22), we investigated whether the loss of *OCLN* expression in 786-O cells could be due to histone modifications. Regarding the *GAS1* gene, we could not observe any change in its expression after the 5-Aza-dC and TSA treatments, and therefore, we also investigated if histone modifications could contribute to *GAS1* supression in the absence of DNA hypermethylation or histone deacetylation.

In both cell lines, ChIP followed by qPCR analysis showed that all of the histone modifications were reduced or absent in the promoter regions of *OCLN* and *GAS1*. It was not possible to differentiate the relative occupancy of the marks studied between the healthy and tumor cell lines. The Human Negative Control Primer Set 1 and Human Positive Control Primer Set GAPDH-2 served as negative and positive controls, respectively (Fig. 5).

*microRNA analysis*. We performed stem-loop reverse transcription PCR (RT-qPCR) to quantify miR-122 and miR-34a expression in the 786-O and HaCaT cell lines. The relative expression of miR-122 and miR-34a in the 786-O cells was higher than in the HaCaT cells (Fig. 6). Both microRNAs were significantly overexpressed in tumor tissues when compared to healthy renal tissues. These results suggest that upregulation of miR-122 and miR-34a may be, at least in part, involved in the downregulation of *OCLN* and *GAS1* in ccRCC.

*Immunohistochemistry*. The SLC2A1 protein expression was investigated in ccRCC tissue array by immunohistochemistry. The ccRCC tissues showed a higher expression of the SLC2A1 protein (p<0.0001) relative to the healthy tissues. Fig. 7 shows the SLC2A1 immunoreactivity and the densitometric data.

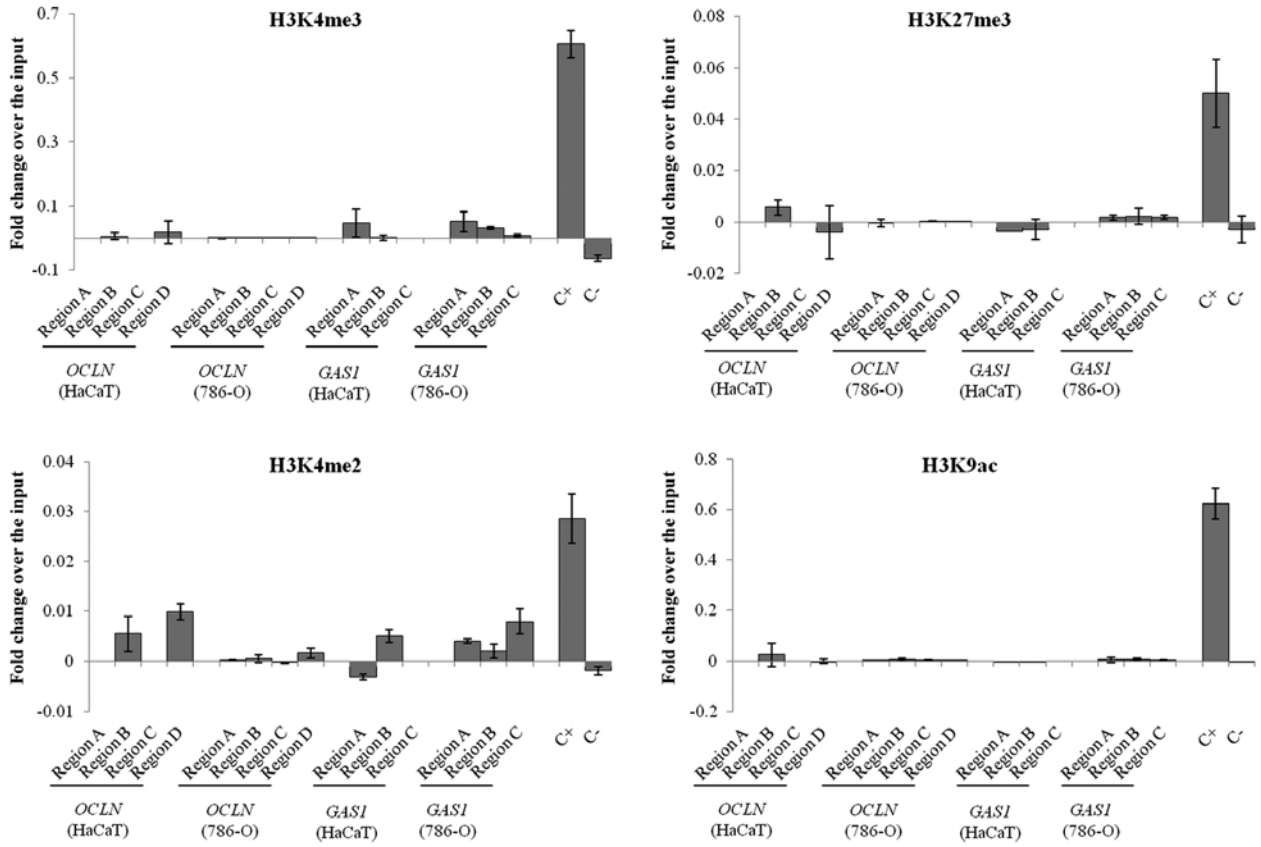


Figure 5. Histone modifications in *OCLN* and *GAS1* gene promoters. ChIP analyses of the levels of H3K4me3, H3K27me3, H3K4me2 and H3K9ac in the *OCLN* and *GAS1* promoter regions. The values are represented as fold-change over the input.

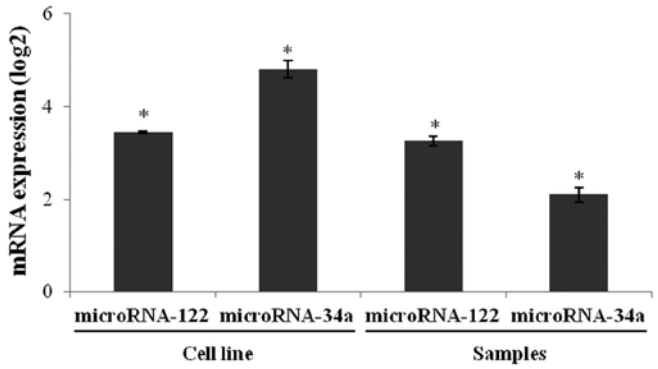


Figure 6. MicroRNA-122 and microRNA-34a expression are upregulated in ccRCC tissues. miR-122 and miR-34a expression levels in the 786-O cell line compared with the HaCaT cell line and the ccRCC samples compared with healthy renal tissue samples (*p<0.001; Wilcoxon signed-rank test).

## Discussion

Several prognostic models are used to predict the survival of ccRCC patients, including clinicopathological parameters and protein, genetic and epigenetic biomarkers (23-25). In the present study, we investigated the epigenetic regulatory mechanisms of *OCLN* and *GAS1*, genes that may contribute to epithelial-mesenchymal transition (EMT), cellular differentiation and proliferation in renal cell carcinoma.

The *OCLN* gene is responsible for producing the occludin protein, which is present in all tight junctions. Occludin has been implicated in tight junction permeability and, in particular, to the regulation of size-selective diffusion (26-28). The transmembrane proteins occludin and claudin are present in tight junctions, which are connected to the cytoskeleton via a network of proteins, such as zonula occludens-1 (29). This epithelial junctional complex, along with adherens junctions and desmosomes, is located at the most apical part of the complex (30). Tight junctions determine epithelial cell polarity and undergo dissolution during cancer progression that is accompanied by cytoskeletal changes (31).

Downregulation of *OCLN* has been observed in liver tumors, breast cancer, endometrial and lung carcinomas (32-35). A study of human cutaneous squamous cell carcinoma observed the loss of OCLN and related this loss to cell-cell adhesion, apoptosis and proliferation (36). *OCLN* was found to be partially methylated in the promoter and endogenous region of a breast cancer cell line, and treatment with 5-Aza-dC and TSA could induce re-expression of this gene (37). In the present study, we observed hypermethylation in ~20% of the endogenous region, although, treatment with 5-Aza-dC did not change the global methylation profile of the *OCLN* gene in the ccRCC cell line. However, we demonstrated that the effect of 5-Aza-dC treatment and the synergistic effect of 5-Aza-dC and TSA treatment in 786-O cells were effective in reactivating *OCLN* gene expression. Thus, 786-O cells showed a methylation profile in the *OCLN* promoter, despite the suggestion of alternate modes of reactivation based upon *OCLN* expression. To further investigate whether increased *OCLN* expression in 786-O cells could be due to chromatin modifications, we

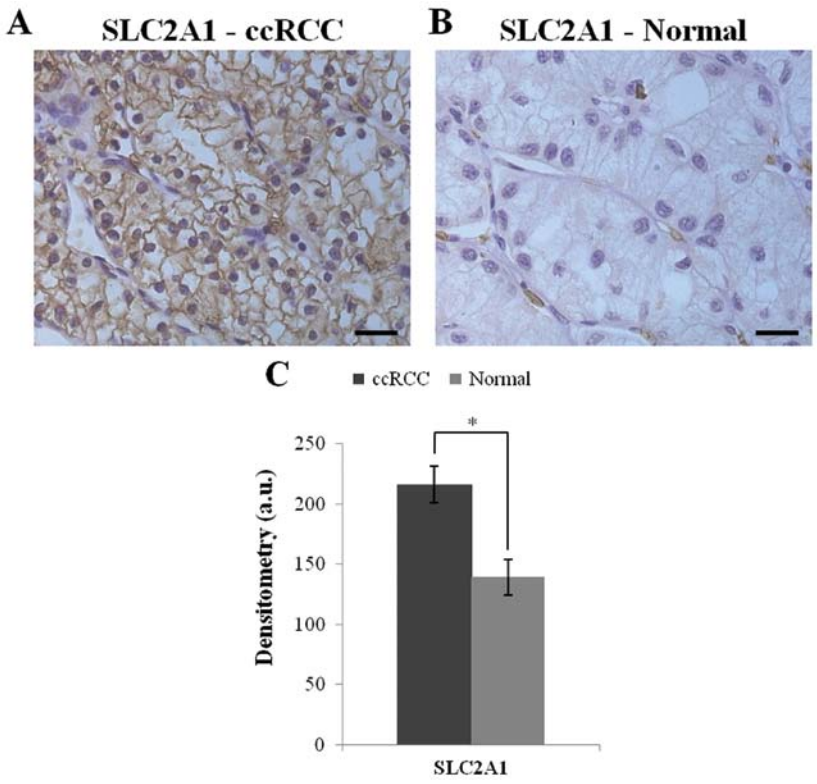


Figure 7. SLC2A1 is highly expressed in ccRCC tissues compared to healthy samples. Protein detection of (A) SLC2A1 in the ccRCC sample. (B) SLC2A1 in a healthy sample. Scale bars, 20 $\mu$m. (C) Histogram of the densitometry of the immunostaining of SLC2A1 in the samples analyzed ($^*p<0.0001$; Mann-Whitney U test).

performed ChIP for H3K27me3, H3K4me3, H3K4me2 and H3K9ac marks in the *OCLN* promoter in 786-O cells. ChIP analysis did not show any differences between H3K27me3 silencing marks or changes in H3K4me3, H3K4me2 and H3K9ac activation marks in the *OCLN* gene promoter region. H3K4me1, H3K4me2 and H3K4me3 marks inform us on the potential prognosis since their increase was found to be inversely correlated with lymph node involvement and distant metastasis in patients with renal cell carcinoma (38).

Another potential regulatory mechanism that may influence *OCLN* expression is microRNAs. miR-122 has been reported to regulate *OCLN* expression in intestinal tissue, which contributes to increased intestinal permeability (39). In the present study, miR-122 expression levels were higher in the ccRCC cell line and tumor samples, suggesting that the increase in microRNA expression may contribute to the downregulation of the *OCLN* gene. miR-122 expression was upregulated in 15 cases of clear cell papillary renal cell carcinoma and in 80 samples of ccRCC (40-42). In breast cancer, high miR-122 levels have been associated with metastasis, likely by increasing nutrient availability in the pre-metastatic niche (43).

GAS1 is a membrane-associated protein; it is tethered to the membrane through a glycosyl-phosphatidylinositol anchor (44,45). GAS1 contributes to inhibitory signal transduction and interferes with cell proliferation due to the inhibition of DNA synthesis during the G0 to S phase (44,46). The Hedgehog pathway is an essential regulator of carcinogenesis, and the GAS1 protein participates in the Hedgehog signaling pathway through the binding to Hedgehog ligands and enhancing the signaling, thus, indirectly inducing EMT (14,47,48).

Reduced *GAS1* expression was found to be positively associated with the survival time in gastric cancer cells (49). The downregulation of the *GAS1* gene has been described in colorectal cancer, melanoma and prostate cancer metastasis (50-52).

In the present study, the global methylation profile of *GAS1* in ccRCC cells was unchanged before and after 5-Aza-dC treatment. Similarly, there were no gene expression modifications after treatment with TSA or co-treatment with TSA and 5-Aza-dC. Sacilotto *et al* (53) suggested that *GAS1* gene transcription is modulated by chromatin remodeling and histone modifying complex recruitment to the *GAS1* promoter in hepatic cells. However, our chromatin immunoprecipitation assays did not show a difference in the H3K27me3 silencing mark, nor were there differences in the H3K4me3, H3K4me2 and H3K9ac activation marks in the *GAS1* gene promoter region in ccRCC cells. It is possible that other regulatory mechanisms are altering the expression of *GAS1* in ccRCC, such as microRNAs.

*GAS1* gene regulation in papillary thyroid carcinoma occurs through miR-34a, leading to cell proliferation and apoptotic suppression (54). miR-34a regulates mesangial proliferation and glomerular hypertrophy by directly inhibiting *GAS1* in early diabetic nephropathies (55). In the present study, we measured miR-34a expression levels, which target the *GAS1* gene, in ccRCC cell lines and tumor samples and suggest that the increase in this microRNA may contribute to the downregulation of *GAS1*. miR-34a was upregulated in 8 ccRCC samples and renal carcinoma cell lines, establishing

an association between this miR and multiple targets (56,57). miR-34a overexpression supports cell proliferation in the majority of cancers, suggesting an unexpected link between cancer and neuronal and endocrine cell metabolism (58).

The *SLC2A1* gene is overexpressed in different types of cancers, including lung, liver and breast (59-61). SLC2A1 facilitates glucose transport and is present in the epithelium and endothelium, contributing to proliferation (59,62,63). In the present study, *SLC2A1* was upregulated in ccRCC samples and 786-O cells as determined by both qPCR and immunohistochemistry. Cifuentes *et al* (64) demonstrated that SLC2A1 and glucose transport are regulated by insulin and therefore may be an important target for conventional pharmaceutical therapy and gene therapy in the treatment of osteosarcoma. The SLC2A1 protein belongs to a class of markers that can detect breast cancer by molecular imaging with more common immunoreactivity in ductal carcinoma *in situ* than in invasive breast cancer (65,66).

In summary, the silencing of *OCLN* and *GAS1* may contribute to tumor progression due to a possible relationship between these genes and cell-cell adhesion, apoptosis and proliferation. We suggest that the increase in miR-122 and miR-34a expression may contribute to the downregulation of the *OCLN* and *GAS1* genes, respectively. Overexpression of the *SLC2A1* gene was higher in ccRCC than that in the non-neoplastic samples. The expression of these genes may be involved in ccRCC progression in addition to other cellular processes that contribute to tumor development. Once these genes have been characterized in ccRCC, molecular genetic tools may be used to explore the biological process involved, thus improving diagnosis, treatment and patient outcomes. More studies should be conducted to assess the overall importance of epigenetic events in the regulation of *OCLN* and *GAS1* expression in ccRCC and in others tumors, as well as its relevancce in the analysis of possible transcription factors that may also contribute to the regulation of the expression of these genes.

## Acknowledgements

The present study was supported by the São Paulo State Research Foundation, FAPESP (2012/08853-0), and the National Council for Research, CNPq.

## References

1. Shuch B, Amin A, Armstrong AJ, Eble JN, Ficarra V, Lopez-Beltran A, Martignoni G, Rini BI and Kutikov A: Understanding pathologic variants of renal cell carcinoma: Distilling therapeutic opportunities from biologic complexity. Eur Urol 67: 85-97, 2015.
2. Cohen HT and McGovern FJ: Renal-cell carcinoma. N Engl J Med 353: 2477-2490, 2005.
3. Kuroda N, Hosokawa T, Michal M, Hes O, Sima R, Ohe C and Lee GH: Clear cell renal cell carcinoma with focal renal angiomyoadenomatous tumor-like area. Ann Diagn Pathol 15: 202-206, 2011.
4. Nagata M, Sakurai-Yageta M, Yamada D, Goto A, Ito A, Fukuhara H, Kume H, Morikawa T, Fukayama M, Homma Y, *et al*: Aberrations of a cell adhesion molecule CADM4 in renal clear cell carcinoma. Int J Cancer 130: 1329-1337, 2012.
5. Baylin SB: DNA methylation and gene silencing in cancer. Nat Clin Pract Oncol 2 (Suppl 1): S4-S11, 2005.
6. Tang J and Zhuang S: Epigenetics in acute kidney injury. Curr Opin Nephrol Hypertens 24: 351-358, 2015.
7. Baylin SB and Ohm JE: Epigenetic gene silencing in cancer - a mechanism for early oncogenic pathway addiction? Nat Rev Cancer 6: 107-116, 2006.
8. Feinberg AP and Tycko B: The history of cancer epigenetics. Nat Rev Cancer 4: 143-153, 2004.
9. Benard A, Goossens-Beumer IJ, van Hoesel AQ, de Graaf W, Horati H, Putter H, Zeestraten EC, van de Velde CJ and Kuppen PJ: Histone trimethylation at H3K4, H3K9 and H4K20 correlates with patient survival and tumor recurrence in early-stage colon cancer. BMC Cancer 14: 531, 2014.
10. Khakpour G, Pooladi A, Izadi P, Noruzinia M and Tavakkoly Bazzaz J: DNA methylation as a promising landscape: A simple blood test for breast cancer prediction. Tumour Biol 36: 4905-4912, 2015.
11. Li J and Mansmann UR: A microRNA molecular modeling extension for prediction of colorectal cancer treatment. BMC Cancer 15: 472, 2015.
12. De Wever O, Pauwels P, De Craene B, Sabbah M, Emami S, Redeuilh G, Gespach C, Bracke M and Berx G: Molecular and pathological signatures of epithelial-mesenchymal transitions at the cancer invasion front. Histochem Cell Biol 130: 481-494, 2008.
13. Pierucci-Alves F, Yi S and Schultz BD: Transforming growth factor beta 1 induces tight junction disruptions and loss of transepithelial resistance across porcine vas deferens epithelial cells. Biol Reprod 86: 36, 2012.
14. Katoh Y and Katoh M: Hedgehog signaling, epithelial-to-mesenchymal transition and miRNA (Review). Int J Mol Med 22: 271-275, 2008.
15. Kunkel M, Reichert TE, Benz P, Lehr HA, Jeong JH, Wieand S, Bartenstein P, Wagner W and Whiteside TL: Overexpression of Glut-1 and increased glucose metabolism in tumors are associated with a poor prognosis in patients with oral squamous cell carcinoma. Cancer 97: 1015-1024, 2003.
16. Sun L, Zeng X, Yan C, Sun X, Gong X, Rao Y and Yan N: Crystal structure of a bacterial homologue of glucose transporters GLUT1-4. Nature 490: 361-366, 2012.
17. Sasaki H, Shitara M, Yokota K, Hikosaka Y, Moriyama S, Yano M and Fujii Y: Overexpression of GLUT1 correlates with *Kras* mutations in lung carcinomas. Mol Med Rep 5: 599-602, 2012.
18. Li W, Wei Z, Liu Y, Li H, Ren R and Tang Y: Increased 18F-FDG uptake and expression of Glut1 in the EMT transformed breast cancer cells induced by TGF-beta. Neoplasma 57: 234-240, 2010.
19. Fisseler-Eckhoff A: New TNM classification of malignant lung tumors 2009 from a pathology perspective. Pathologe 30 (Suppl 2): S193-S199, 2009 (In German).
20. Pfaffl MW: A new mathematical model for relative quantification in real-time RT-PCR. Nucleic Acids Res 29: e45, 2001.
21. Calmon MF, Colombo J, Carvalho F, Souza FP, Filho JF, Fukuyama EE, Camargo AA, Caballero OL, Tajara EH, Cordeiro JA, *et al*: Methylation profile of genes *CDKN2A* (*p14* and *p16*), *DAPK1*, *CDH1*, and *ADAM23* in head and neck cancer. Cancer Genet Cytogenet 173: 31-37, 2007.
22. Nguyen CT, Weisenberger DJ, Velicescu M, Gonzales FA, Lin JC, Liang G and Jones PA: Histone H3-lysine 9 methylation is associated with aberrant gene silencing in cancer cells and is rapidly reversed by 5-aza-2'-deoxycytidine. Cancer Res 62: 6456-6461, 2002.
23. Zigeuner R, Hutterer G, Chromecki T, Imamovic A, Kampel-Kettner K, Rehak P, Langner C and Pummer K: External validation of the Mayo Clinic stage, size, grade, and necrosis (SSIGN) score for clear-cell renal cell carcinoma in a single European centre applying routine pathology. Eur Urol 57: 102-109, 2010.
24. Gulati S, Martinez P, Joshi T, Birkbak NJ, Santos CR, Rowan AJ, Pickering L, Gore M, Larkin J, Szallasi Z, *et al*: Systematic evaluation of the prognostic impact and intratumour heterogeneity of clear cell renal cell carcinoma biomarkers. Eur Urol 66: 936-948, 2014.
25. Fisel P, Kruck S, Winter S, Bedke J, Hennenlotter J, Nies AT, Scharpf M, Fend F, Stenzl A, Schwab M, *et al*: DNA methylation of the *SLC16A3* promoter regulates expression of the human lactate transporter MCT4 in renal cancer with consequences for clinical outcome. Clin Cancer Res 19: 5170-5181, 2013.
26. Furuse M, Hirase T, Itoh M, Nagafuchi A, Yonemura S, Tsukita S and Tsukita S: Occludin: A novel integral membrane protein localizing at tight junctions. J Cell Biol 123: 1777-1788, 1993.

27. Balda MS, Whitney JA, Flores C, González S, Cereijido M and Matter K: Functional dissociation of paracellular permeability and transepithelial electrical resistance and disruption of the apical-basolateral intramembrane diffusion barrier by expression of a mutant tight junction membrane protein. J Cell Biol 134: 1031-1049, 1996.
28. Balda MS, Flores-Maldonado C, Cereijido M and Matter K: Multiple domains of occludin are involved in the regulation of paracellular permeability. J Cell Biochem 78: 85-96, 2000.
29. Tsukita S, Furuse M and Itoh M: Multifunctional strands in tight junctions. Nat Rev Mol Cell Biol 2: 285-293, 2001.
30. Farquhar MG and Palade GE: Junctional complexes in various epithelia. J Cell Biol 17: 375-412, 1963.
31. Thiery JP and Sleeman JP: Complex networks orchestrate epithelial-mesenchymal transitions. Nat Rev Mol Cell Biol 7: 131-142, 2006.
32. Orbán E, Szabó E, Lotz G, Kupcsulik P, Páska C, Schaff Z and Kiss A: Different expression of occludin and ZO-1 in primary and metastatic liver tumors. Pathol Oncol Res 14: 299-306, 2008.
33. Martin TA, Mansel RE and Jiang WG: Loss of occludin leads to the progression of human breast cancer. Int J Mol Med 26: 723-734, 2010.
34. Tobioka H, Isomura H, Kokai Y, Tokunaga Y, Yamaguchi J and Sawada N: Occludin expression decreases with the progression of human endometrial carcinoma. Hum Pathol 35: 159-164, 2004.
35. Tobioka H, Tokunaga Y, Isomura H, Kokai Y, Yamaguchi J and Sawada N: Expression of occludin, a tight-junction-associated protein, in human lung carcinomas. Virchows Arch 445: 472-476, 2004.
36. Rachow S, Zorn-Kruppa M, Ohnemus U, Kirschner N, Vidal-y-Sy S, von den Driesch P, Börnchen C, Eberle J, Mildner M, Vettorazzi E, *et al*: Occludin is involved in adhesion, apoptosis, differentiation and $Ca^{2+}$-homeostasis of human keratinocytes: Implications for tumorigenesis. PLoS One 8: e55116, 2013.
37. Osanai M, Murata M, Nishikiori N, Chiba H, Kojima T and Sawada N: Epigenetic silencing of occludin promotes tumorigenic and metastatic properties of cancer cells via modulations of unique sets of apoptosis-associated genes. Cancer Res 66: 9125-9133, 2006.
38. Ellinger J, Kahl P, Mertens C, Rogenhofer S, Hauser S, Hartmann W, Bastian PJ, Büttner R, Müller SC and von Ruecker A: Prognostic relevance of global histone H3 lysine 4 (H3K4) methylation in renal cell carcinoma. Int J Cancer 127: 2360-2366, 2010.
39. Ye D, Guo S, Al-Sadi R and Ma TY: MicroRNA regulation of intestinal epithelial tight junction permeability. Gastroenterology 141: 1323-1333, 2011.
40. Munari E, Marchionni L, Chitre A, Hayashi M, Martignoni G, Brunelli M, Gobbo S, Argani P, Allaf M, Hoque MO, *et al*: Clear cell papillary renal cell carcinoma: micro-RNA expression profiling and comparison with clear cell renal cell carcinoma and papillary renal cell carcinoma. Hum Pathol 45: 1130-1138, 2014.
41. White NM, Bao TT, Grigull J, Youssef YM, Girgis A, Diamandis M, Fatoohi E, Metias M, Honey RJ, Stewart R, *et al*: miRNA profiling for clear cell renal cell carcinoma: Biomarker discovery and identification of potential controls and consequences of miRNA dysregulation. J Urol 186: 1077-1083, 2011.
42. Zhou L, Chen J, Li Z, Li X, Hu X, Huang Y, Zhao X, Liang C, Wang Y, Sun L, *et al*: Integrated profiling of microRNAs and mRNAs: microRNAs located on Xq27.3 associate with clear cell renal cell carcinoma. PLoS One 5: e15224, 2010.
43. Fong MY, Zhou W, Liu L, Alontaga AY, Chandra M, Ashby J, Chow A, O'Connor ST, Li S, Chin AR, *et al*: Breast-cancer-secreted miR-122 reprograms glucose metabolism in premetastatic niche to promote metastasis. Nat Cell Biol 17: 183-194, 2015.
44. Ruaro ME, Stebel M, Vatta P, Marzinotto S and Schneider C: Analysis of the domain requirement in Gas1 growth suppressing activity. FEBS Lett 481: 159-163, 2000.
45. Stebel M, Vatta P, Ruaro ME, Del Sal G, Parton RG and Schneider C: The growth suppressing *gas1* product is a GPI-linked protein. FEBS Lett 481: 152-158, 2000.
46. Del Sal G, Ruaro ME, Philipson L and Schneider C: The growth arrest-specific gene, *gas1*, is involved in growth suppression. Cell 70: 595-607, 1992.
47. Beachy PA, Karhadkar SS and Berman DM: Tissue repair and stem cell renewal in carcinogenesis. Nature 432: 324-331, 2004.
48. Allen BL, Tenzen T and McMahon AP: The Hedgehog-binding proteins Gas1 and Cdo cooperate to positively regulate Shh signaling during mouse development. Genes Dev 21: 1244-1257, 2007.
49. Wang H, Zhou X, Zhang Y, Zhu H, Zhao L, Fan L, Wang Y, Gang Y, Wu K, Liu Z, *et al*: Growth arrest-specific gene 1 is downregulated and inhibits tumor growth in gastric cancer. FEBS J 279: 3652-3664, 2012.
50. Jiang Z, Xu Y and Cai S: Down-regulated *GAS1* expression correlates with recurrence in stage II and III colorectal cancer. Hum Pathol 42: 361-368, 2011.
51. Gobeil S, Zhu X, Doillon CJ and Green MR: A genome-wide shRNA screen identifies *GAS1* as a novel melanoma metastasis suppressor gene. Genes Dev 22: 2932-2940, 2008.
52. Scaltriti M, Brausi M, Amorosi A, Caporali A, D'Arca D, Astancolle S, Corti A and Bettuzzi S: Clusterin (SGP-2, ApoJ) expression is downregulated in low- and high-grade human prostate cancer. Int J Cancer 108: 23-30, 2004.
53. Sacilotto N, Espert A, Castillo J, Franco L and López-Rodas G: Epigenetic transcriptional regulation of the *growth arrest-specific gene 1* (*Gas1*) in hepatic cell proliferation at mononucleosomal resolution. PLoS One 6: e23318, 2011.
54. Ma Y, Qin H and Cui Y: MiR-34a targets GAS1 to promote cell proliferation and inhibit apoptosis in papillary thyroid carcinoma via PI3K/Akt/Bad pathway. Biochem Biophys Res Commun 441: 958-963, 2013.
55. Zhang L, He S, Guo S, Xie W, Xin R, Yu H, Yang F, Qiu J, Zhang D, Zhou S, *et al*: Down-regulation of miR-34a alleviates mesangial proliferation in vitro and glomerular hypertrophy in early diabetic nephropathy mice by targeting GAS1. J Diabetes Complications 28: 259-264, 2014.
56. Liu H, Brannon AR, Reddy AR, Alexe G, Seiler MW, Arreola A, Oza JH, Yao M, Juan D, Liou LS, *et al*: Identifying mRNA targets of microRNA dysregulated in cancer: With application to clear cell renal cell carcinoma. BMC Syst Biol 4: 51, 2010.
57. Yu G, Li H, Wang J, Gumireddy K, Li A, Yao W, Tang K, Xiao W, Hu J, Xiao H, *et al*: miRNA-34a suppresses cell proliferation and metastasis by targeting CD44 in human renal carcinoma cells. J Urol 192: 1229-1237, 2014.
58. Dutta KK, Zhong Y, Liu YT, Yamada T, Akatsuka S, Hu Q, Yoshihara M, Ohara H, Takehashi M, Shinohara T, *et al*: Association of microRNA-34a overexpression with proliferation is cell type-dependent. Cancer Sci 98: 1845-1852, 2007.
59. Yan S, Wang Y, Chen M, Li G and Fan J: Deregulated SLC2A1 promotes tumor cell proliferation and metastasis in gastric cancer. Int J Mol Sci 16: 16144-16157, 2015.
60. Amann T, Maegdefrau U, Hartmann A, Agaimy A, Marienhagen J, Weiss TS, Stoeltzing O, Warnecke C, Schölmerich J, Oefner PJ, *et al*: *GLUT1* expression is increased in hepatocellular carcinoma and promotes tumorigenesis. Am J Pathol 174: 1544-1552, 2009.
61. Krzeslak A, Wojcik-Krowiranda K, Forma E, Jozwiak P, Romanowicz H, Bienkiewicz A and Brys M: Expression of GLUT1 and GLUT3 glucose transporters in endometrial and breast cancers. Pathol Oncol Res 18: 721-728, 2012.
62. Manel N, Kim FJ, Kinet S, Taylor N, Sitbon M and Battini JL: The ubiquitous glucose transporter GLUT-1 is a receptor for HTLV. Cell 115: 449-459, 2003.
63. Augustin R: The protein family of glucose transport facilitators: It's not only about glucose after all. IUBMB Life 62: 315-333, 2010.
64. Cifuentes M, García MA, Arrabal PM, Martínez F, Yañez MJ, Jara N, Weil B, Domínguez D, Medina RA and Nualart F: Insulin regulates GLUT1-mediated glucose transport in MG-63 human osteosarcoma cells. J Cell Physiol 226: 1425-1432, 2011.
65. Vermeulen JF, van Brussel AS, van der Groep P, Morsink FH, Bult P, van der Wall E and van Diest PJ: Immunophenotyping invasive breast cancer: Paving the road for molecular imaging. BMC Cancer 12: 240, 2012.
66. Vermeulen JF, van der Wall E, Witkamp AJ and van Diest PJ: Analysis of expression of membrane-bound tumor markers in ductal carcinoma in situ of the breast: Paving the way for molecular imaging. Cell Oncol 36: 333-340, 2013.